Catal Lett
DOI 10.1007/s10562-013-1063-x

PdAu Alloy Nanoparticles Encapsulated by PPI-g-MWCNTs as a Novel Catalyst for Chemoselective Hydrogenation of Alkenes Under Mild Conditions

Ahmad Shaabani · Mojtaba Mahyari

Received: 5 May 2013 / Accepted: 1 July 2013

Abstract The synthesis, characterization and catalytic applications of bimetallic PdAu encapsulated on polypropylene imine grafted multi-wall carbon nanotubes hybrid materials have been reported. The results show that the catalyst induces a highly activity and chemoselective hydrogenation of less hindered alkenes to the corresponding alkanes using hydrogen gas in environmentally friendly solvents H_2O/EtOH at 50 °C with high yields. The characterization of catalyst was confirmed by FT-IR, transmission electron microscopy, X-ray photoelectron spectroscopy, and X-ray powder diffraction.

Keywords Bimetallic · Polypropylene imine · Multi-wall carbon nanotubes · Chemoselective hydrogenation

1 Introduction

The selective hydrogenation is a critical step in the synthesis of chemical intermediates that have wide applications in many fields such as foods, pharmaceuticals, cosmetics, plastics, and lubricants industries [1–3]. Encapsulated noble metals are industrial and academic important catalytic for the selective hydrogenation [4, 5]. Bimetallic nanoparticles (NPs) have appeared as an important class of catalysts. Bimetallic nanoparticles based on the mixing pattern, can be divided into three main types [6]. Heterostructures, core–shell structures, and intermetallic or alloyed structures. Among these types, bimetallic alloy NPs are very important nanomaterials because of their applications in large variety of catalytic reactions, including catalytic alcohol oxidation, reforming reactions, and pollution control [7–11]. The addition of a second metal is an important approach for tailoring the geometric and electronic structures of NPs to promote their catalytic activity and selectivity.

Carbon nanotubes (CNTs) are attractive solid supports for heterogeneous catalysts due to their unique properties and surface structures [12], but there are some difficulties in dispersing metal nanoparticles on the surface of pristine CNTs.

In this work, a well-defined polymer known as dendrimer [13, 14] is used as template to control the size, stability, and solubility of nanoparticles ranging in diameter from <1 to 5 nm. Dendrimers are suitable for hosting metal nanoparticles especially for catalytic systems due to the following reasons: (i) the nanoparticles are stabilized by encapsulation within the dendrimer, and they do not agglomerate [15–21]; (ii) the encapsulated nanoparticles are confined by steric effects, and therefore a substantial fraction of their surface is unpassivated and available to take part in catalytic reactions [16, 17, 19–21]; (iii) moreover, the dendrimer branches can be employed as selective gates to control access of small substrates to the encapsulated nanoparticles and therefore inducing selectivity to the reaction.

In continuation our research program on the catalytic transformation of organic compounds [22–25], herein, we report the synthesis of supported bimetallic PdAu nanoparticles via co-complexation method on first, second, and third generation of polypropylene imine grafted multi-wall carbon nanotubes (PPI-g-MWCNTs) for hydrogenation of

---

Electronic supplementary material The online version of this article (doi:10.1007/s10562-013-1063-x) contains supplementary material, which is available to authorized users.

A. Shaabani (✉) · M. Mahyari
Department of Chemistry, Shahid Beheshti University,
G. C., P.O. Box 19396-4716, Tehran, Iran
e-mail: a-shaabani@sbu.ac.ir

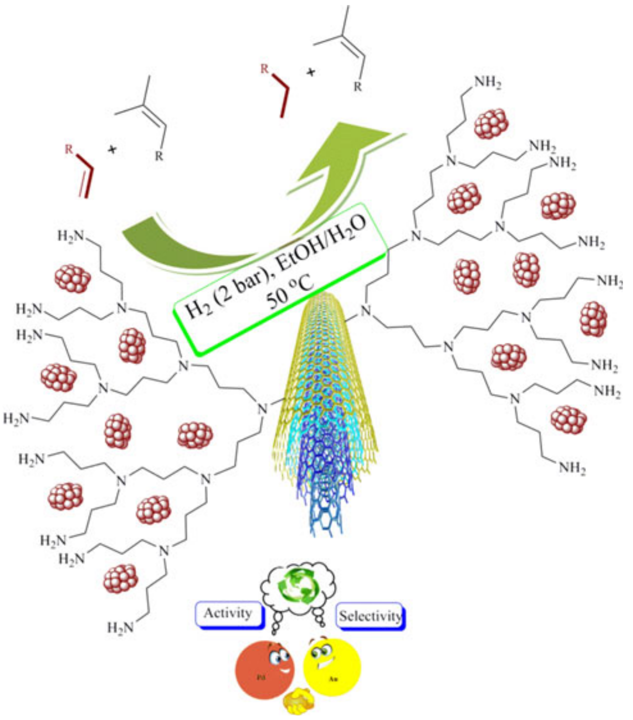

Scheme 1 Selective hydrogenation of alkenes by bimetallic PdAu nanoparticles encapsulated by PPI-g-MWCNTs

alkenes. The results show that catalyst induces a highly chemoselective hydrogenation of less hindered alkenes to the corresponding alkanes under mild conditions with high yields. The entire concept is summarized in Scheme 1 graphically.

2 Experimental

2.1 Materials

MWCNTs were prepared by chemical vapour deposition procedure in the presence of Co/Mo/MgO as a catalyst at 900 °C [26]. The outer diameter of MWCNTs was between 20 and 40 nm. All solvents and reagents were purchased from Aldrich or Merck and used without further purification.

2.2 Instruments and Characterization

^{1}H NMR spectra were recorded with a BRUKER DRX-300 AVANCE spectrometer, and $CDCl_3$ was used as a solvent. IR spectra were recorded on a Bomem MB-Series FT-IR spectrophotometer. A transmission electron microscopy (TEM) analysis was performed by LEO 912AB electron microscope. Identification and quantification were carried out on a Varian model 3600 gas chromatograph (Varian Iberica, Madrid, Spain) equipped with a split/splitless capillary injection port and flame ionization detector (FID). A CP-Sil-8 fused silica capillary column (25 m–0.32 mm i.d. and 0.52 mm film thickness) from Chrompack was employed. X-ray photoelectron spectroscopy (XPS) analysis was performed using a VG multilab 2000 spectrometer (ThermoVG scientific) in an ultra high vacuum. Catalysis products were analysed using a Varian 3900 GC (GC conversion was obtained using n-decane as an internal standard based on the amount of arylhalide employed relative to authentic standard product). Ultrasonic bath (EUROSONIC® 4D ultrasound cleaner with a frequency of 50 kHz and an output power of 350 W) was used to disperse materials in solvent. Thermogravimetric analysis (TGA) was carried out using STA 1500 instrument at a heating rate of 10 °C min^{-1} in air. X-ray powder diffraction (XRD) data were collected on an XD-3A diffractometer using Cu Kα radiation.

2.2.1 *Preparation of MWCNTs–COCl*

Typically 0.6–1.0 g of purified MWCNTs–COOH species was stirred in a mixture of 160.0–200.0 mL $SOCl_2$ and 20.0 mL DMF at 80 °C for 50 h. The MWCNTs–COCl was isolated by vacuum filtration through a PTFE membrane (pore size 0.2 mm) and washed with dry methylene chloride. Usually MWCNTs–COCl was used almost immediately after isolation in the next reaction step in order to avoid the hydrolysis of it [27].

2.2.2 *Curtius Rearrangement for the Synthesis of MWCNTs–NH_2*

MWCNTs–COCl (1.0 g) and NaN_3 (2.0 g, 30 mmol) were stirred in 800.0 mL DMF at room temperature for 30 h. Then the temperature was raised up to 100 °C and stirring continued for an additional 20 h. The reaction product was isolated by filtration, and after 10 h sonication in conc. hydrochloric acid yielded MWCNTs–NH_2 [13].

2.2.3 *Preparation of PPI-Grafted-MWCNTs Hybrid Materials*

First-, second- and third-generation PPI dendrimers were synthesized on the amino functionalized MWCNTs. The amino functionalized MWCNTs (0.8 g) was added in portions at ambient temperature with stirring to acrylonitrile (3.4 mL, 80 mmol) and methanol (10.0 mL) in a 100 mL round-bottomed flask. The reaction mixture was stirred at ambient temperature under nitrogen atmosphere for 5 days. After the completion of reaction, excess reactants and solvent were removed under vacuum. The product was washed with MeOH and CH_2Cl_2. It was dried under vacuum for 24 h. Then, $CoCl_2 \cdot 6H_2O$ (23.8 g, 100 mmol) in MeOH (300.0 mL) and $NaBH_4$ (19.0 g, 500 mmol) were added to the product of previous step; the mixture was stirred at 20 °C for 24 h. After that, the mixture was acidified with 3 N HCl (100.0 mL). Next, the product was filtered under vacuum, washed with ethanol and water and dried under vacuum at 50 °C for 4 h. Then the synthesis, titration method [28] was used to calculate the amount of free primary amines in the periphery of the dendrimers (Table 1) [13, 29].

2.2.4 *Preparation of Bimetallic PdAu Dendrimer-Encapsulated Catalyst*

First, aqueous solution of $PdCl_2$ (0.1 g in 3.0 mL) and PPI-g-MWCNTs (0.2 g in 10.0 mL) were mixed and placed in an ultrasonic bath (50 kHz) for 20 min to well disperse metal ions in the dendritic shell of hybrid materials. Then, the mixture was stirred for 30 min, aqueous solution of $HAuCl_4$ (0.2 g in 3.0 mL) was added. The solution was placed in an ultrasonic bath for 20 min, followed by addition of 10.5 mL of a 1.0 M $NaBH_4$ solution in 0.3 M aqueous NaOH [17, 30]. After stirring for several hours, it was filtered under vacuum, washed well with ethanol and water and dried under vacuum at 50 °C for 4 h.

2.3 General Catalytic Hydrogenation

A 10 mL Ace glass pressure tube was loaded with 0.008 g of third generation PPI-g-MWCNTs (0.2 mol% Pd, 0.2 mol% Au) and 1 mmol of each alkene with 2.0 mL mixture H_2O/EtOH (1:1) and then pressurized to 2 bar with molecular hydrogen (H_2) as a hydrogen source. The pressure tube was placed in an oil bath thermostated at 50 °C to initiate the reaction. Aliquots of the organic phase were analyzed by gas chromatography using a CP-Sil-8 fused silica capillary column.

3 Results and Discussion

3.1 Synthesis and Characterization of Supported Catalyst

Polyamidoamine (PAMAM) [17, 31] and polypropyleneimine (PPI) dendrimers are the most widely used dendrimers in various applications, but we chose PPI because they are stable at very high temperatures, whereas PAMAM dendrimers undergo retro-Michael addition at temperatures higher than about 100 °C [32]. We used carbon nanotube as support because they may also act a role in the hydrogenation processes. Kim et al. [33] reported that when hydrogen gas is in contact with multiwalled carbon nanotubes (MWCNTs) attached with Ni nanoparticles, the formation of atomic hydrogen is possible. Although the reasons are not well understood, experimental evidence supports the fact that CNT-supported metallic nanoparticles introduce a new class of recyclable and efficient catalysts for chemical syntheses specially for catalytic hydrogenation reactions. The chemical modification of MWCNTs with first, second and third generation of PPI and subsequent loading of palladium and gold has been outlined in Schemes 2 and 3. The direct attachment of amino groups to SWCNTs opened edges was reported by Gromov and co-workers [27]. First, Curtius rearrangement for the synthesis of MWCNTs–$CONH_2$ was carried out. Amino functionalized MWCNT undergoes Michael addition with acrylonitrile and subsequently the cobalt (II)-catalyzed reduction of the nitrile group to produce first generation of PPI-g-MWCNTs. The above step has been repeated to synthesis of second and third generation of PPI-g-MWCNTs. The FT-IR spectra of each generation PPI-g-MWCNTs were shown in Fig. 1. The broad band at 3,418 cm^{-1} is due to the –NH_2 stretching, the absorption at 1,605 cm^{-1} is attributed to the N–H bending of the amine groups and the bands at 1,360–1,370 cm^{-1} could be assigned to the C–N stretching of amine groups. The bands at 3,000–3,048 cm^{-1} are assigned to the C–H stretching. The increase in the relative intensity of the above absorptions indicates that each generation of dendrimer was successfully constructed on the surface of MWCNTs.

^{1}H NMR results provide valuable information on the functional groups in the third generation PPI-g-MWCNTs samples in $CDCl_3$. The hydrogen signals of the grafted dendritic units are obviously observable in the corresponding ^{1}H NMR spectrum. The most shielded signal at 1.35 ppm is attributed to $CH_2CH_2CH_2$ and the next signal at 1.7 ppm could be assigned to CH_2N. The peak at 7.6 ppm was assigned to NH_2 groups (Fig. S1).

The titration method was used for the quantification of the growth of the dendrimers on the surface MWCNTs. The calculated amount of –NH_2 groups on each generation of the PPI-g-MWCNTs hybrid materials was shown in Table 1.

Finally, bimetallic palladium-gold dendrimer-encapsulated catalyst has been prepared by the co-complexation

Table 1 Amount of –NH_2 groups and Pd(0) and Au(0) on each generation of the PdAu Ns-PPI-g-MWCNTs hybrid materials

Entry	Generation	–NH_2 content[a] (mmol g^{-1})	Amount of Au(0)[b] (mmol g^{-1})	Amount of Pd(0)[b] (mmol g^{-1})
1	0	0.28	0.11	0.20
2	1	0.41	0.19	0.32
3	2	0.72	0.52	0.80
4	3	1.08	0.90	1.72

[a] Determined by titration method

[b] Determined by AAS

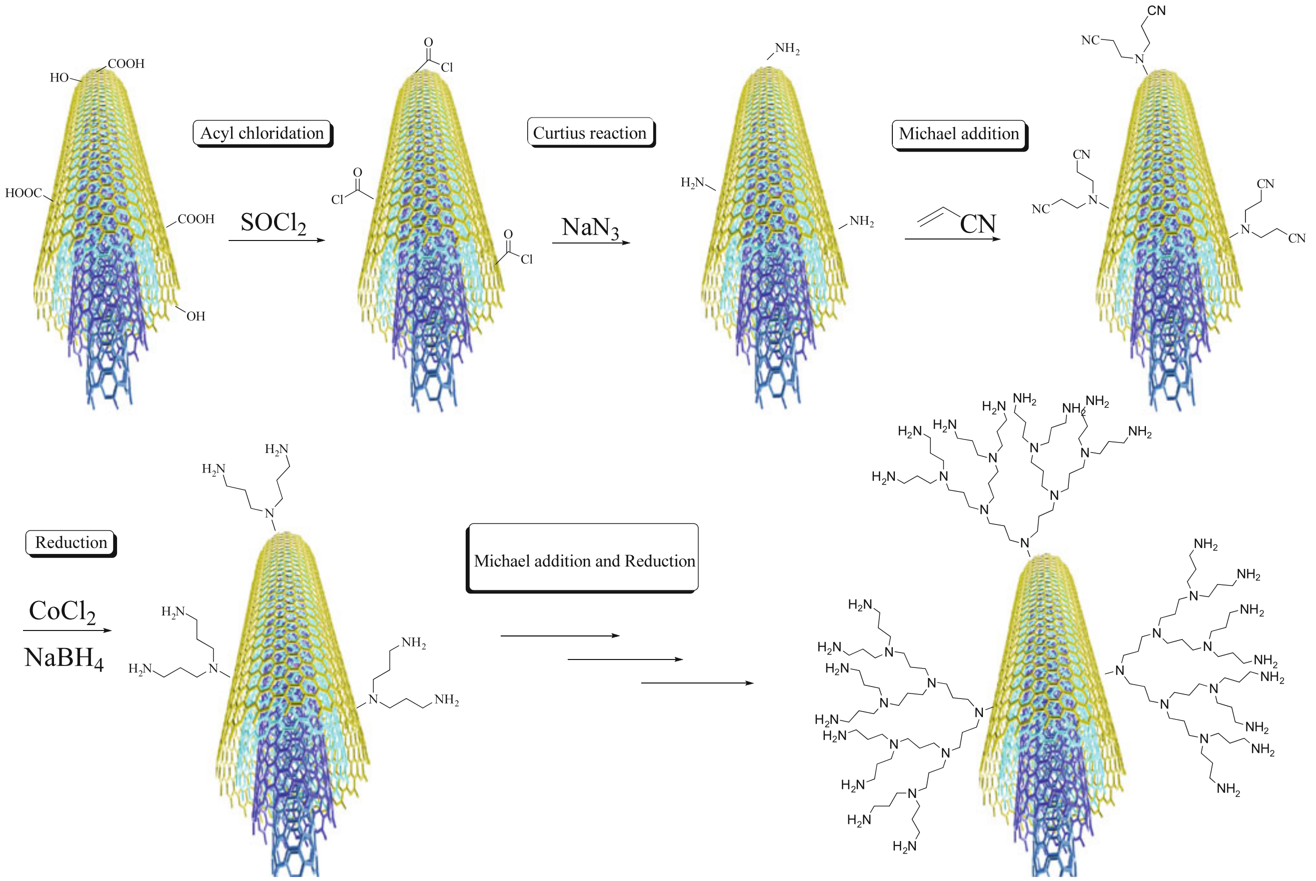

Scheme 2 Synthesis route of carbon nanotube-supported poly(propylene imine) dendrimer

method [34]. Atomic absorption spectroscopy (AAS) determined the amount of Pd and Au in each generation (Table 1). As the generation of PPI rose, the loading of Pd and Au nanoparticles was increased. This can be attributed to an exponential increase of amino groups with the increase in the generation of dendrimer.

TEM of third generation PPI-g-MWCNTs contained PdAu bimetallic nanoparticles and also showed the nanoparticles uniformly dispersed on MWCNTs (Fig. S2A, B). Figure S2c shows the size distribution of encapsulated palladium and gold bimetallic nanoparticles in the dendritic shell of PPI-g-MWCNTs.

XPS data of the third generation of the bimetallic PdAu nanoparticles PPI-g-MWCNTs showed about a 1:1 ratio of PdAu content in the catalyst with 18.3 wt% Pd (1.7 mmol Pd(0)/g catalyst) and 17.8 wt% Au (0.89 mmol Au(0)/g catalyst) which are in good agreement with AAS results. XPS spectra of the PdAu catalyst revealed the presence of Pd($3d_{5/2}$) and Pd($3d_{3/2}$) peaks at 335.4 and 340.8 eV and Au($4f_{7/2}$) and Au($4f_{5/2}$) peaks at 84.0 and 87.8 eV, respectively (Fig. S3). These binding energy values are in accordance with those reported for metallic Pd(0) and Au(0) oxidation states.

The nitrogen (N 1s) signals are due to PPI produced during the synthesis of PdAu Ns-PPI-g-MWCNTs hybrid materials.

As shown in Fig. 2, the XRD pattern of third generation of PPI-g-MWCNTs PdAu nanoparticles indicated a peak for the Pd with a 2θ value of about 39.24°, 45.46° and 66.19° and well-defined peaks of the Au nanoparticles with 2θ values of 35.74°, 47.76°, 63.19°, 79.78°. The broad peaks at $2\theta = 23.27°$ are relative to the (002) planes of the graphite like structure of the multi-walled carbon nanotubes [35]. According to literature, the spectrum of monometallic Au reveled two sharp scattering peaks at 38.2° and 44.4°, which are assigned to (111) and (200) planes, respectively. The monometallic Pd revealed one peak centering at about 40.119°, which is identified as the (111) plane palladium. Our catalyst (PdAu Ns-PPI (G3)-g-MWCNTs hybrid materials) revealed scattering peaks at 39.24° and 45.46° which are very close to the peak positions of (111) and (200) planes of gold. The position of the first peak clearly indicates an intermediate scattering angle between those of the monometallic nanoparticles. Consequently, it was found that alloying of the two metal atoms was taking place throughout. These results are consistent with previous reports of gold–

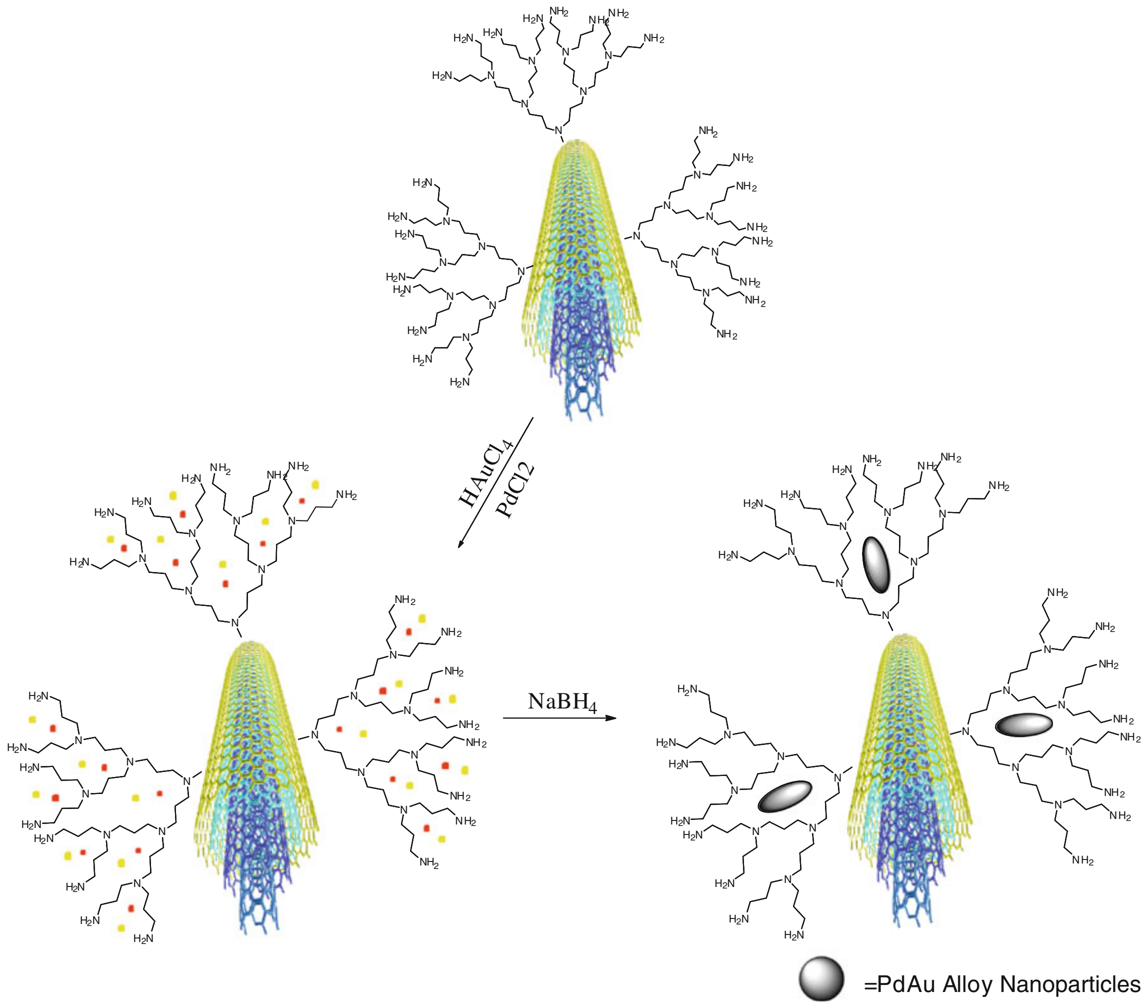

Scheme 3 Synthesis route of PdAu Ns-PPI-g-MWCNTs hybrid materials

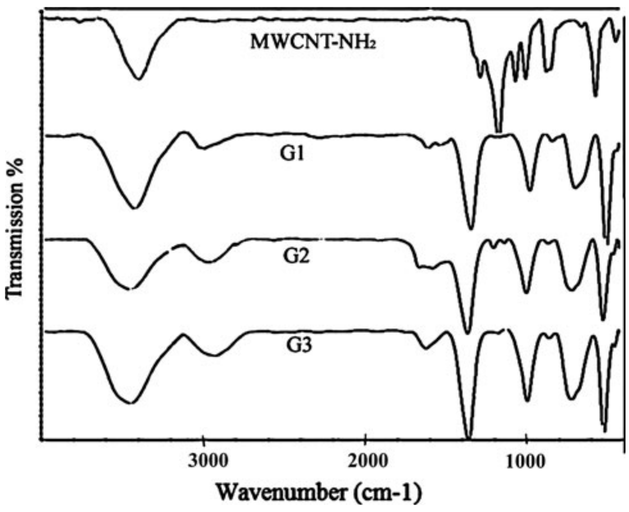

Fig. 1 FT-IR spectra for carbon nanotube-supported dendrimer

palladium alloy nanoparticles in which the XRD peaks were found to lie between those of pure gold and pure palladium nanoparticles [36]. Moreover, according to Scherrer's equation, it implies that the crystallite size is 1.9 nm for PdAu alloy nanoparticles which is in good agreement with TEM results. Considering the results obtained from XPS, XRD, and also the synthesis method (co-complexation method) of the nanoparticles no core–shell structure observed [34, 36–38].

3.2 The Catalytic Activity of PdAu Ns-PPI-g-MWCNTs Toward the Hydrogenation Reaction

To evaluate the catalytic properties of the catalyst, hydrogenation reaction of cyclohexene was performed as a model reaction. Since Au atoms draw electron density away from Pd atoms, thereby enhancing the interaction of

Pd atoms with olephin, the large efficiency for the bimetallic materials is observed. Such synergistic interactions have also been reported for PdPt and PdRh DECs [39–42].

The reaction was carried out in the presence of various amounts of catalyst. As the catalyst amount was increased (0.008 g), the reaction went to completion more rapidly at 50 °C. After screening a variety of solvents, mixed H_2O/EtOH was determined to be the best solvents that was used due to coincidence to green chemistry principle. The temperature of the reaction plays an important role, increasing the temperature to 50 °C on the aqueous solvent provided higher conversion. The best results were obtained in the presence of 0.008 g of catalyst in mixed H_2O/EtOH (1:1, 2 mL) at 50 °C (Tables 2, 3).

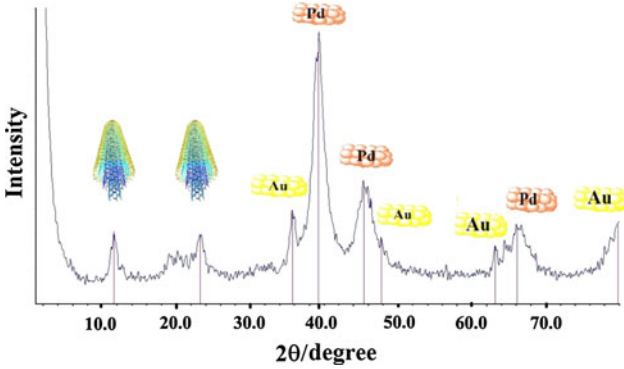

Fig. 2 X-ray diffraction (XRD) pattern of PdAu Ns-PPI (G3)-g-MWCNTs hybrid materials

The first, second, and third generation catalysts was investigated for hydrogenation reaction of various alkenes under 2 bar pressure of hydrogen gas at 50 °C. As indicated in Table 2, the third generation catalyst shows the most activity and selectivity for chemoselective hydrogenation of less hindered alkenes. As indicated in Fig. 3, the sterically hindered alkenes did not undergo hydrogenation; this was verified by competition reaction between cyclohexene/1-methylcyclohexene with PdAu Ns-PPI (G3)-g-MWCNTs catalyst.

CNTs are attractive solid supports for heterogeneous catalysts due to their unique properties and surface structures [12, 43–45]. Kim et al. [33] reported the possibility formation of atomic hydrogen on MWCNTs attached with Ni nanoparticles. Although the reasons are not well understood, experimental evidences support the fact that CNT-supported metallic nanoparticles introduce a new class of recyclable and efficient catalysts for chemical syntheses especially for catalytic hydrogenation reactions. We tested activity of MWCNT, PPI (G3)-g-MWCNTs and PdAu Ns-MWCNTs. As shown in the Table 3 entries 1–3, the MWCNT and PPI (G3)-g-MWCNTs without using metals indicate little activity in the hydrogenation reaction, but PdAu Ns-MWCNTs shows relatively good activity but due to hydrophobic nature of CNT and its tendency for agglomeration, we have to use as dendrimer to overcome these problems [46–49]. Moreover, the existence of dendrimer induce more selectivity to our system, because as mentioned before the dendrimer branches can be employed

Table 2 Chemoselective hydrogenation of various alkenes with generations of catalyst

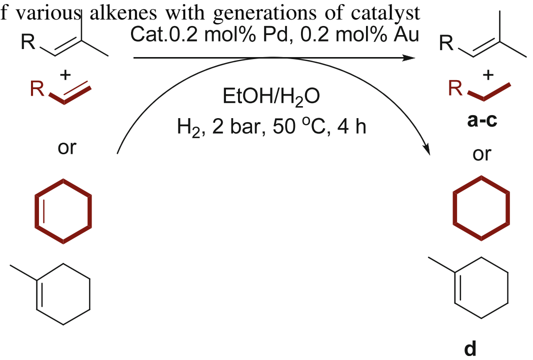

Entry	R	Less hindered (yield %)[a]			More hindered (yield %)[a]		
		G1	G2	G3	G1	G2	G3
a	C_4H_9	82	90	>99	12	5	<2
b	C_6H_{13}	88	92	>95	10	3	<5
c	C_6H_5	90	94	>98	15	7	<4
d	–	89	94	>99	5	<3	0

Reaction conditions: 1.00 mmol of each alkene, catalyst (0.008 g), EtOH/H_2O (2 mL), H_2 (2 bar) at 50 °C for 4 h

[a] Yield determined by GC analysis

Table 3 Comparison of PPI (G3)-g-MWCNTs, PdAu Ns-PPI (G3)-g-MWCNTs, and monometallic counterparts as catalyst for hydrogenation reaction

Entry	Catalyst	Yield (%)[a]	
		Less hindered	More hindered
1	MWCNTs	8	6
2	PdAu Ns-MWCNTs	65	10
3	PPI (G3)-g-MWCNTs	9	8
4	Au Ns-PPI (G3)-g-MWCNTs	72	<2
5	Pd Ns-PPI (G3)-g-MWCNTs	78	20
6	PdAu Ns-C	70	4
7	PdAu Ns-PPI (G3)-g-MWCNTs	>99	0

Reaction conditions: cyclohexene (1.00 mmol), 1-methylcyclohexene (1.00 mmol), EtOH/H_2O (2 mL), H_2 (2 bar) at 50 °C for 4 h

[a] Yield determined by GC analysis

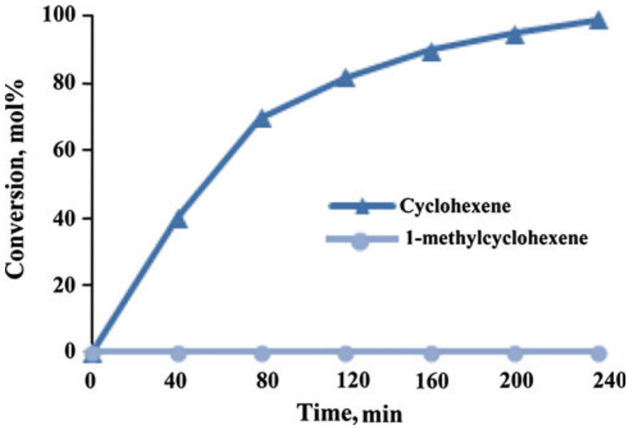

Fig. 3 Reaction profile for competitive hydrogenation of cyclohexene with 1-methylcyclohexene with PdAu Ns-PPI (G3)-g-MWCNTs

as selective gates to control access of small substrates to the encapsulated nanoparticles and therefore inducing selectivity to the reaction.

To confirm the activity and efficiency of PdAu Ns-PPI (G3)-g-MWCNTs catalyst relative to corresponding individual nanoparticles (Pd or Au) catalysts and also to investigate the effect of support, hydrogenation reaction of mixed cyclohexene and 1-methylcyclohexene as a model reaction was examined. As indicated in Table 3, owing to strong synergy between the metals, the catalytic hydrogenation of alkenes was significantly enhanced in the presence of bimetallic alloy NPs than their monometallic counterparts (Table 3, entries 4, 5 and 7). The gold catalysts exhibit much lower activity than the group VIII in dissociation of H_2 [50] and it is strongly dependent on the amount of low coordination sites available on the gold nanoparticles and is thus favoured when the size of the particles decreases [51, 52]. Moreover, experimental results shows that the presence of gold nanoparticles enhance the selectivity of catalyst. Palladium nanoparticles lead to higher yields relative to gold nanoparticles but with lower selectivity (entries 4 and 5). Therefore, the combination of gold and palladium in an alloy nanoparticle configuration is an efficient way to enhance catalytic activity and selectivity [32, 33] (entries 4 and 5).

The combination of gold and palladium in an alloy nanoparticle configuration was an efficient way to enhanced catalytic activity due to the geometric and electronic effects [32, 33]. In addition, to investigate the advantages of new catalyst over the AuPd immobilized on other supports, we used activated carbon, which the results presented more activity and selectivity for PdAu Ns-PPI (G3)-g-MWCNTs, because as previously mentioned dendritic structures induce narrow size distribution of very small nanoparticles and also the dendrimer branches can be employed as selective gates to control access of small substrates to the encapsulated nanoparticles and therefore inducing selectivity to the reaction.

When heterogeneous catalyst is used, the leaching of active metal species into solution is an important issue that should be considered. In a separate experiment, the catalyst was filtered off after ~50 % conversion under the reaction conditions. The AAS analysis of the filtrate also confirmed that the Pd and Au content in the solution were below the detection limit (0.1 ppm). But since testing the filtrate for Au and Pd may show no metal as they plate out onto the reactor surface, we analyse the Au and Pd concentrations of PdAu Ns-PPI (G3)-g-MWCNTs catalyst especially after the 6 uses which contained 0.77 mmol g^{-1} Pd(0) and 0.5 mmol g^{-1} Au(0). So the leaching of Pd and Au after 6 uses was negligible.

The recyclability and reusability of the PdAu Ns-PPI-g-MWCNTs catalyst was tested for the hydrogenation reaction mixed of cyclohexene and 1-methylcyclohexene up to

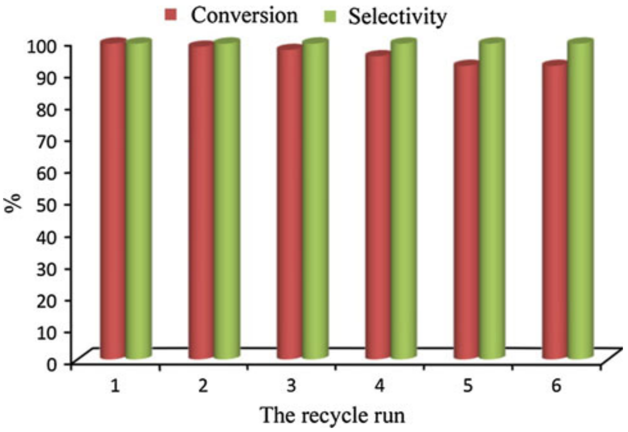

Fig. 4 Effect of recycling on the catalytic efficiency of PdAu Ns-PPI (G3)-g-MWCNTs

six cycles. The results in Fig. 4 demonstrate that after every run, the yield and selectivity of reaction does not change significantly; this finding shows the stability of catalyst under experimental conditions.

4 Conclusions

In summary, first, second and third generation of PPI-g-MWCNTs were successfully synthesized and PdAu nanoparticles encapsulated on this surface. Highly dispersed PdAu Ns-PPI (G3)-g-MWCNTs hybrid materials showed high chemoselectivity and activity for hydrogenation of less hindered alkenes in mild and environmentally friendly conditions. Due to the simplicity and non-hazardous nature of the catalyst, it could be used in a variety of experiments also the catalyst can be used several times without significant loss of activity and selectivity.

Acknowledgments We gratefully acknowledge financial support from the Catalysis Center of Excellence (CCE) at Shahid Beheshti University.

References

1. Al-Herz M, Simmons MJ, Wood J (2011) Ind Eng Chem Res 51:8815–8825
2. Edwards JK, Carley AF, Herzing AA, Kiely CJ, Hutchings GJ (2008) Faraday Discuss 138:225–239
3. Blaser HU, Steiner M, Studer H (2009) ChemCatChem 1:210–221
4. Durand J, Teuma E, Gómez M (2008) Eur J Inorg Chem 2008:3577–3586
5. Kwon MS, Kim N, Park CM, Lee JS, Kang KY, Park J (2005) Org Lett 7:1077–1079
6. Wang D, Li Y (2011) Adv Mater 23:1044–1060
7. Jiang H-L, Xu Q (2011) J Mater Chem 21:13705–13725
8. Ji X, Lee KT, Holden R, Zhang L, Zhang J, Botton GA, Couillard M, Nazar LF (2010) Nat Chem 2:286–293
9. Jiang H-L, Akita T, Ishida T, Haruta M, Xu Q (2011) J Am Chem Soc 133:1304–1306
10. Studt F, Abild-Pedersen F, Bligaard T, Sørensen RZ, Christensen CH, Nørskov JK (2008) Science 320:1320–1322
11. Tee Y-H, Grulke E, Bhattacharyya D (2005) Ind Eng Chem Res 44:7062–7070
12. Yoon B, Wai CM (2005) J Am Chem Soc 127:17174–17175
13. Buhleier E, Wehner W, Vögtle F (1978) Synthesis 2:155–158
14. Bosman AW, Janssen HM, Meijer EW (1999) Chem Rev 99:1665–1688
15. Zhao M, Sun L, Crooks RM (1998) J Am Chem Soc 120:4877–4878
16. Zhao M, Crooks RM (1999) Angew Chem Int Ed Engl 38:364–366
17. Crooks RM, Zhao M (1999) Adv Mater 11:217–220
18. Zhao M, Crooks RM (1999) Chem Mater 11:3379–3385
19. Yeung LK, Crooks RM (2001) Nano Lett 1:14–17
20. Chechik V, Zhao M, Crooks RM (1999) J Am Chem Soc 121:4910–4911
21. Chechik V, Crooks RM (2000) J Am Chem Soc 122:1243–1244
22. Shaabani A, Rahmati A, Badri Z (2008) Catal Commun 9:13–16
23. Shaabani A, Maleki A (2007) Appl Catal A 331:149–151
24. Shaabani A, Farhangi E, Rahmati A (2008) Appl Catal A 338:14–19
25. Shaabani A, Farhangi E (2009) Appl Catal A 371:148–152
26. Yeoh W-M, Lee K-Y, Chai S-P, Lee K-T, Mohamed AR (2009) New Carbon Mater 24:119–123
27. Gromov A, Dittmer S, Svensson J, Nerushev OA, Perez-García SA, Licea-Jiménez L, Rychwalski R, Campbell EE (2005) J Mater Chem 15:3334–3339
28. Kapoor MP, Kasama Y, Yokoyama T, Yanagi M, Inagaki S, Nanbu H, Juneja LR (2006) J Mater Chem 16:4714–4722
29. Moors R, Vögtle F (1993) Chem Ber 126:2133–2135
30. Gröhn F, Bauer BJ, Akpalu YA, Jackson CL, Amis EJ (2000) Macromolecules 33:6042–6050
31. Zhao M, Tokuhisa H, Crooks RM (1997) Angew Chem Int Ed Engl 36:2596–2598
32. Zhao M, Liu Y, Crooks RM, Bergbreiter DE (1999) J Am Chem Soc 121:923–930
33. Kim H-S, Lee H, Han K-S, Kim J-H, Song M-S, Park M-S, Lee J-Y, Kang J-K (2005) J Phys Chem B 109:8983–8986
34. Scott RW, Wilson OM, Oh S-K, Kenik EA, Crooks RM (2004) J Am Chem Soc 126:15583–15591
35. Guo G, Qin F, Yang D, Wang C, Xu H, Yang S (2008) Chem Mater 20:2291–2297
36. Han Y-F, Zhong Z, Ramesh K, Chen F, Chen L, White T, Tay Q, Yaakub SN, Wang ZJ (2007) Phys Chem C 111:8410–8413
37. Oh S-K, Kim Y-G, Ye H, Crooks RM (2003) Langmuir 19:10420–10425
38. Kim Y-G, Oh S-K, Crooks RM (2004) Chem Mater 16:167–172
39. Kim JH, Bryan WW, Chung H-W, Park CY, Jacobson AJ, Lee TR (2009) ACS Appl Mater Interfaces 1:1063–1069
40. Scott RWJ, Datye AK, Crooks RM (2003) J Am Chem Soc 125:3708–3709
41. Chung Y-M, Rhee H-K (2003) Catal Lett 85:159–164
42. Chung Y-M, Rhee H-K (2003) J Mol Catal A Chem 206:291–298
43. Pan H-B, Yen CH, Yoon B, Wai CM (2006) Synth Commun 36:3473–3478
44. Yoon B, Sheaff CN, Eastwood D, Wai CM (2007) J Nanophoton 1:013508
45. Eastwood D, Femandez C, Yoon B, Sheaff CN, Wai CM (2006) Appl Spectrosc 60:958–963
46. Krishnan GR, Sreekumar K (2008) Eur J Org Chem 2008: 4763–4768
47. Jiang Y, Jiang J, Gao Q, Ruan M, Yu H, Qi L (2008) Nanotechnology 19:075714
48. Hagiwara H, Sasaki H, Tsubokawa N, Hoshi T, Suzuki T, Tsuda T, Kuwabata S (2010) Synlett 2010:1990–1996
49. Hwang SH, Moorefield CN, Wang P, Jeong KU, Cheng SZD, Kotta KK, Newkome GR (2006) J Am Chem Soc 128:7505–7509
50. Stobinski L, Zommer L, Dus R (1999) Appl Surf Sci 141:319–325
51. Bus E, Miller JT, Bokhoven JA (2005) J Phys Chem B 109:14581–14587
52. Bus E, Prins R, Bokhoven JA (2007) Phys Chem Chem Phys 9:3312–3320